ARTICLE

Carbon Nanotube Doping Mechanism in a Salt Solution and Hygroscopic Effect: Density Functional Theory

Dinh Loc Duong,[†] Il Ha Lee,[†] Ki Kang Kim,[‡] Jing Kong,[‡] Seung Mi Lee,[§] and Young Hee Lee[†,*]

[†]Sungkyunkwan Advanced Institute of Nanotechnology, Department of Energy Science, Center for Nanotubes and Nanostructured Composites, Sungkyunkwan University, Suwon 440-746, Republic of Korea, [‡]Department of Electrical Engineering & Computer Science, Massachusetts Institute of Technology, Cambridge, Massachusetts 02139, and [§]Center for Materials Measurement, Korea Research Institute of Standards and Science, Daejeon 305-340, Republic of Korea

ABSTRACT The mechanism of doping carbon nanotubes (CNTs) with a salt solution was investigated using the density functional theory. We propose that the anion—CNT complex is a key component in doping CNTs. Although the cations play an important role in ionizing CNTs as an intermediate precursor, the ionized CNTs are neutralized further by forming a stable anion—CNT complex as a final reactant. The anion—CNT bond has a strong ionic bonding character and clearly shows p-type behavior by shifting the Fermi level toward the valence band. The midgap state is introduced by the strong binding of carbon and anion atoms. These localized charged anion sites are highly hygroscopic and induce the adsorption of water molecules. This behavior provides a new possibility for using anion-functionalized CNTs as humidity sensors.

KEYWORDS: carbon nanotube · doping mechanism · density functional theory · salt solution · hygroscopic effect

Tailoring the electronic properties of carbon nanotubes (CNTs) is an important step for many applications including nanotransistors, nanosensors, and thin conducting films.[1−6] To modify the electronic structures of CNTs, numerous studies on the doping of CNTs have been performed. There are three main doping strategies: endohedral doping, in-plane doping, and exohedral doping.[1] Endohedral doping can be accomplished using C_{60} in peapod structures or by metallocence.[7] In in-plane doping, boron or nitrogen atoms are often used to substitute carbon atoms on the CNT wall to produce p-type or n-type semiconductors, respectively.[1,8] In exohedral doping, many types of organic as well as inorganic molecules can be employed for doping the CNTs by chemical adsorption as well as physical absorption on the CNT surface.[7,9−11] Among the three doping strategies mentioned above, exohedral doping is the most robust method because many types of atoms and molecules can be chosen, including alkaline, halogen, and organic molecules and solvents as charge dopants.

Recently, a new strategy for controlling the doping type depending on the redox potential was introduced.[12] A chemical with a higher reduction potential than that of CNT is regarded as an acceptor when it extracts electrons from the CNTs, and a chemical with a lower reduction potential than that of CNT is considered a donor because it is able to donate electrons to the CNTs. For instance, the reduction potential of benzyl viologen (BV) is −1.1 V *vs* SHE, which is below the reduction potential of CNT (+0.5 V *vs* SHE). Therefore, electrons are donated from viologen to CNT, and viologen acts as an n-type dopant.[11] Likewise, 2,3-dichloro-5,6-dicyano-*p*-benzoquinone (DDQ) is a p-type doping agent. These behaviors have been confirmed both by experiments and by first-principle density functional theory (DFT) calculations.[12−14]

Compared to the direct adsorption of organic molecules on the CNT surface, doping of CNTs by salt solutions such as $AuCl_3$, Na_2PtCl_4, and $NOBF_4$ has a different reaction mechanism. In this case, a direct redox reaction occurs between the CNTs and the salt solution. Because of the higher reduction potential, cations in solution have a tendency to receive electrons from the CNTs. Due to charge transfer, positive ions such as Au^{3+}, Pt^{2+}, and NO^+ cations are reduced to metal clusters or gas.[15] In turn, the CNTs accumulate positive charges and show p-type behavior. The charged CNTs can be stable in the ionic liquid due to solvation. The question of stability arises when the doped CNTs are dry but still show p-type behavior.[6] In this case, the charged CNTs are not stable and, therefore, need to be neutralized further. The origin of stable p-type CNTs has not been clearly explained.

*Address correspondence to leeyoung@skku.edu.

Received for review May 24, 2010 and accepted July 29, 2010.

Published online August 4, 2010.
10.1021/nn1011489

© 2010 American Chemical Society

CNTs are a good candidate for gas sensor applications due to their high surface areas. Two main mechanisms have been proposed to explain the changes in conductance and capacitance, particularly for AC measurements: charge transfers between gas molecules and the CNTs that change the conductance and quantum capacitance of the CNTs, and polarization of the gas.[2,4] Because of the hydrophobic nature of the CNT surface, the CNT transport is rather insensitive to humidity.[16] It is known that pure single-walled nanotubes (SWCNTs) with a PMMA substrate are rather insensitive to humidity, although SWCNTs with an oxide substrate are highly sensitive to humidity.[17] Charge transfer between H_2O molecules and a CNT has been reported to be negligible from theoretical calculations.[18−23] Recently, a strong hygroscopic effect has been observed in a $AuCl_3$-doped CNT device, although the origin of this effect has not been clarified.[29]

The purpose of this paper is two-fold: (i) identify the final state of the CNT complex with salt solution doping that leads to p-type behavior and(ii) determine the hygroscopic origin of the resulting CNTs. In this paper, we used DFT calculations to investigate the salt solution doping mechanism of the CNTs. We propose that Au^{3+} ions are reduced to Au^0 as a precursor, and a CNT−Cl complex is formed to give rise to p-type doping in the CNTs. We found that this CNT−Cl complex plays an important role in the experimentally observed hygroscopic effect.

RESULTS AND DISCUSSION

Mechanism of Doping CNTs with a Salt Solution. Gold chloride has been commonly utilized to demonstrate the doping effect on CNTs.[6,15] Gold clusters have been observed on the CNT surface after the reaction. Au^{3+} can be easily reduced to Au^0 by extracting electrons from the CNTs, which leaves the CNTs positively charged. This is ascribed to the larger reduction potential of Au^{3+} compared to that of the CNTs. The formation of Au nanoparticles on the CNT surface has been observed in SEM images, confirming the reduction reaction of the Au ions.[6,15] In this case, CNTs are positively charged and can be stabilized in the solvent due to solvation. On the other hand, when the doped CNTs are left dry, the charged CNTs are no longer stable in air, and therefore, the charge neutrality condition must be satisfied by further reaction. The G-band of the CNTs in air is upshifted, similar to the behavior in liquid.[6] Hence, we propose here that chlorine ions can be further adsorbed onto the CNT surface during drying, so that the positively charged CNTs can be stabilized by maintaining charge neutrality with the negatively charged chlorine ions. In this case, chlorine-doped CNTs should demonstrate p-type behavior, which is in agreement with experimental observations. A similar phenomenon was also observed with a zinc rod immersed in a copper sulfate ($CuSO_4$) solution. In this case, Cu^{2+} is reduced to Cu^0, which aggregates as clusters on the Zn rod surface. The charged Zn^{2+} rods are then dissolved in the solution. When the water is completely removed, Zn^{2+} and SO_4^{2-} combine together to form $ZnSO_4$.[32]

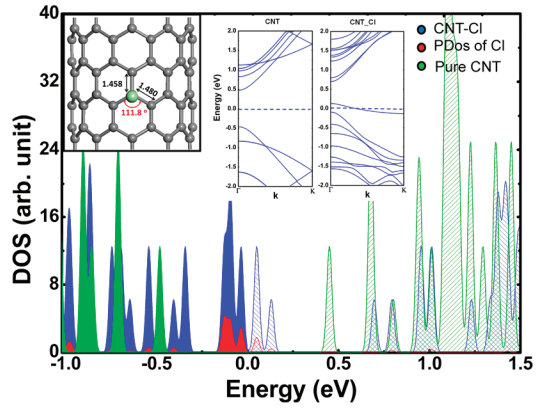

Figure 1. Electronic densities of pure (10,0) CNT and Cl-doped CNT states. The partial densities of the Cl states in the Cl-doped CNTs are also shown. The optimized geometry of the Cl-doped CNT and the band structures of a pure CNT and a Cl-doped CNT (inset) are presented. The valence (conduction) band below (above) the Fermi level (taken as zero) is indicated by the shadow (hatched line).

Figure 1 shows the optimized configuration and band structures (inset), the total electronic densities of the states (DOS), and the partial electronic densities of the states (PDOS) of pure and Cl-doped (10,0) SWCNTs. The binding energy of a Cl atom to the (10,0) CNT is about −0.57 eV with a bond length of 2.11 Å. Here, the negative sign represents an exothermic reaction. The C−C back-bond lengths at the Cl site increase from 1.42 to 1.45 and 1.48 Å. The C−C(Cl)−C bond angles are reduced to 112 from 120°, indicating enhanced sp^3 hybridization by pulling a carbon atom out of the CNT surface. In a bare (10,0) SWCNT, the Fermi level is located in the middle of the gap, which is taken as zero. In a Cl-doped CNT, on the other hand, strong sp^3 hybridization between Cl and a carbon atom in the CNT brings forth a charge transfer and creates nearly midgap states in both occupied and unoccupied states, downshifting the Fermi level, as shown in the band structure. Because of the high electronegativity, it is expected that the Cl atom as well as other halogen atoms can extract electrons from the CNT.[33−37] The Mulliken population analysis shows that 0.22 e^- is extracted from the CNT, consistent with a previous report.[28] Therefore, holes are generated in the CNT, which is congruent with experimental observations of $AuCl_3$ doping. Note that the Fermi levels were all shifted to zero for comparison. Midgap states are contributed mostly from the four carbon atoms near the Cl atom and from the Cl atom itself, as visualized from PDOS. It is intriguing to note that this mid-

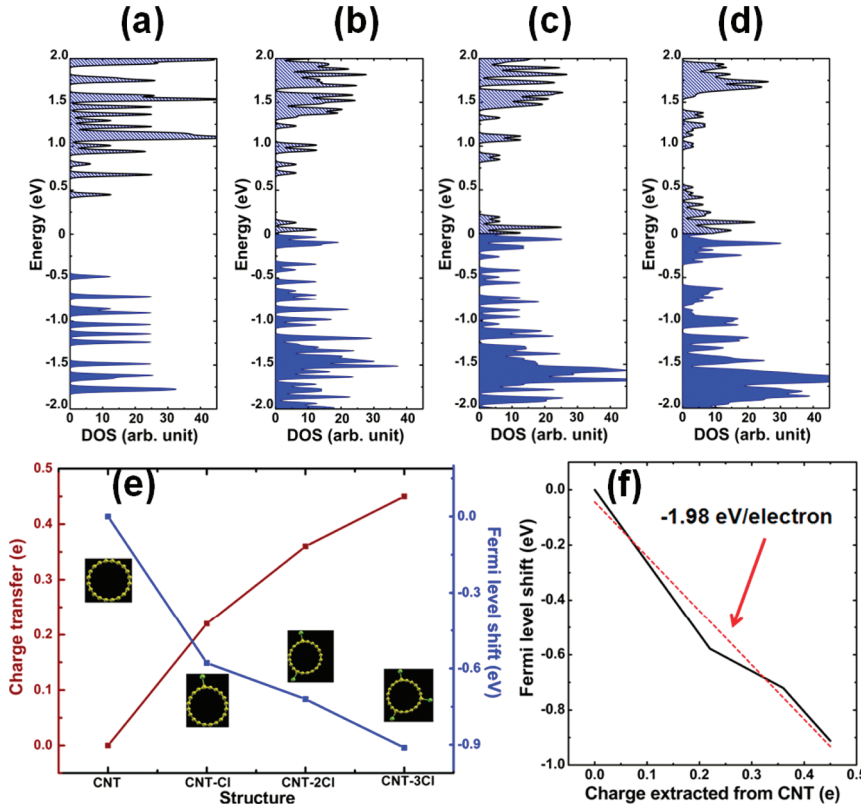

Figure 2. Effects of Cl concentration: (a−d) electronic densities of states of bare (10,0) CNT, (10,0) CNT+Cl, (10,0) CNT+2Cl, (10,0) CNT+3Cl, respectively. (e) Electron transfer and the Fermi level shift (eV) at different chlorine concentrations, and (f) the Fermi level shift *vs* the charges extracted from the CNT.

gap is nearly half filled, as shown in the inset of Figure 1, although interactions between the Cl atoms at a high Cl concentration open the band gap due to repulsive forces between charged Cl atoms, similar to Peierls distortion (Supporting Information S1). Thus, the metallic behavior or small band gap induced by salt solution doping gives rise to an increase in the on-current or an equivalent decrease in the on/off ratio in CNT-based transistors.[29]

Next, the effects of chlorine concentration on the electronic properties of the CNTs were considered. We assumed that Cl atoms were uniformly distributed on the CNT wall. To simplify our model, we introduced two and three chlorine atoms that were uniformly adsorbed onto the CNT wall. Therefore, the strong interactions between Cl atoms can be neglected at low Cl concentrations. The optimized structure and the DOS are shown in Figure 2, and the detailed structural parameters are listed in Table 1. Adding Cl atoms simply increases the DOS near the midgap level. The amount of total charge transfers also increases with increasing number of Cl atoms. Accordingly, the Fermi level is downshifted further, as shown in Figure 2e. Again, this is congruent with the experimentally observed p-type behavior.[6] At high Cl concentrations, however, Cl atoms may interact with each other, giving rise to repulsive forces due to the negatively charged Cl ions. This results in a small band gap (Supporting Information S1). The Fermi level shift with respect to the amount of charge transfer is nearly −1.98 eV/electron, as shown in Figure 2f.

TABLE 1. Electronic Properties of Carbon Nanotubes Doped with Chlorine Atoms at Different Concentrations

	binding energy (eV)	charges extracted from CNT (e^-)	Fermi level (eV)
CNT(10,0)			−4.55
CNT−Cl	−0.57	0.22	−5.13
CNT−Cl_2	−1.06	0.36	−5.27
CNT−Cl_3	−1.65	0.45	−5.46

Gold nanoclusters are a byproduct of the redox reaction, in this circumstance.[6,15] The formation process of Au clusters should be an exothermic process. To confirm this scenario, we first considered three different structures of Au adsorption on the CNT, as shown in Figure 3a. Simple Au^0 adsorption gives a binding energy of −0.33 eV. When a Cl atom is introduced on the top of the Au atom (Figure 3b), the binding energy of the Au is increased to −1.25 eV, illustrating that the adsorption of this Cl−Au complex is much stronger than those of the individual Au and Cl atoms, as shown in Figure 3c. This calculation strongly indicates that Au adsorption is enhanced by the presence of a Cl atom. This opens another possibility that a Au−Cl cluster could be a possible complex to be formed during $AuCl_3$ re-

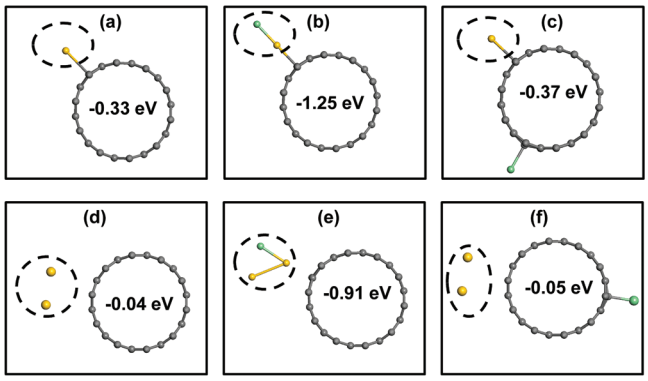

Figure 3. Binding energies of different forms of (a−c) Au atoms and (d−f) Au dimers associated with Cl atoms on the CNT.

action. When two reduced Au atoms are considered, the binding energy is reduced to −0.04 eV (Figure 3d). The additional complex of Cl−Au_2 again increases the binding energy to −0.91 eV (Figure 3e). This value is much larger than those of the individual Au_2 and Cl, as shown in Figure 3f. The binding energy of the Au cluster is enhanced by formation of a complex with Cl atoms. It is intriguing to see the effect of Au adsorption on the electronic structure of the CNT in spite of the enhanced binding energy. The Au contribution to the electronic density of states near the Fermi level was negligible for both cases of a single Au atom and a Au cluster (Supporting Information S2 and S3), in contrast with Cl adsorption, which leads to deep gap states.

Hygroscopic Effect of Cl-Doped CNT. It is known that $HAuCl_4$ (Au^{3+}) and CNT can react together in a water−ethanol solvent.[15] Our calculations predict that the ionic bonding character of the CNT−Cl structure results in high solubility in aqueous solutions. Therefore, the electronic properties of the CNT−Cl structure are expected to be strongly affected by humidity. To consider this effect, we introduced water molecules absorbed at the chlorine site on the CNT surface. The optimized structures and variations of the band structure of the Cl-doped CNT are shown in Figure 4 and are listed in Table 2. In general, the adsorption of water molecules is weak (−0.02 eV) compared to Cl adsorption, as shown in Figure 4b. However, this binding energy is significantly increased to −0.1 eV when a Cl atom is involved (Figure 4c). The binding energy is further increased when more water molecules are adsorbed (Figure 4d). This binding energy increase is ascribed to the strong charge transfer

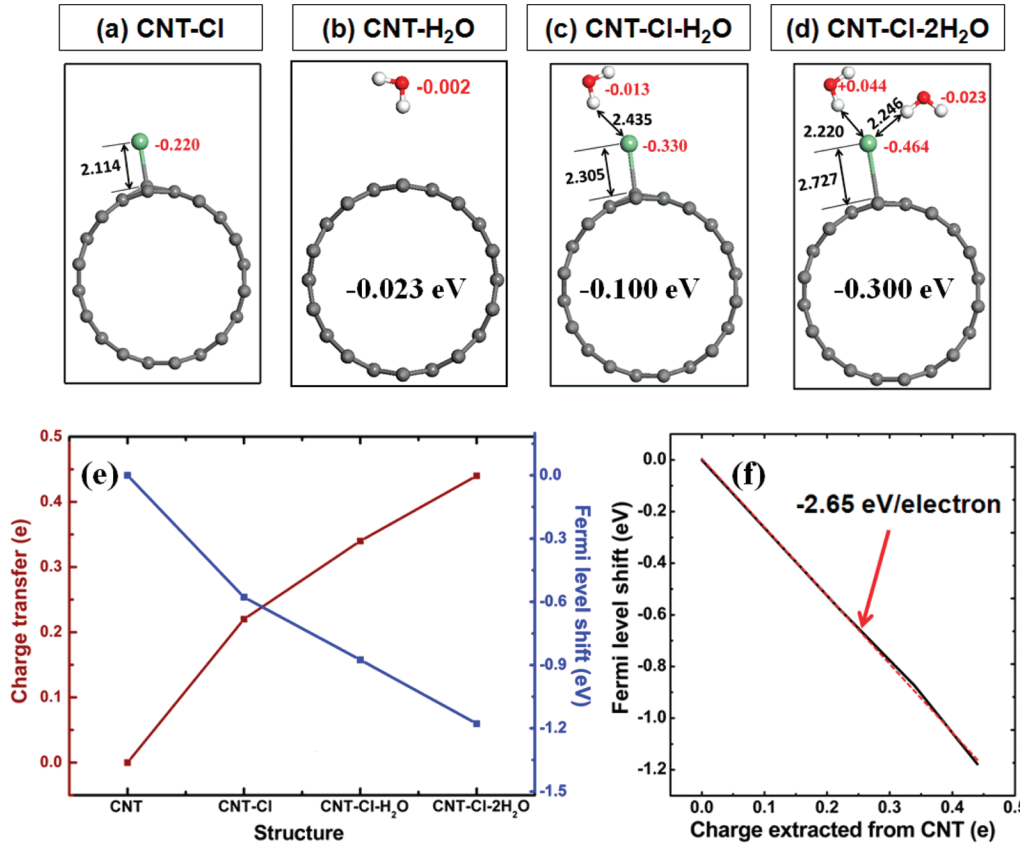

Figure 4. Hygroscopic properties of the Cl−CNT structure. The distance of the C−Cl bond in Å and the local charges in electrons are shown in (a−d) with the binding energy of water molecules. (e) Charge transfer (electron) and the Fermi level shift (eV) as a function of water molecule concentration, and (f) Fermi level *vs* the charges extracted from the CNT are also shown. The adsorption energy of H_2O molecule CNT−Cl structure was defined by $E_{ads} = E_{tot}(CNT-Cl-nH_2O) - E_{tot}(CNT-Cl) - nE_{tot}(H_2O)$. In the case of CNT only, $E_{ads} = E_{tot}(CNT-H_2O) - E_{tot}(CNT) - E_{tot}(H_2O)$.

TABLE 2. Changes in the Electronic Properties of Chlorine-Doped Carbon Nanotubes at Different Humidities: Binding Energy Is Defined by $E_{binding} = E_{total}(CNT+molecules) - E_{tot}(CNT) - E_{tot}(molecules)$

	binding energy (eV)	C−Cl bonding distance (Å)	charges extracted from CNT (e^-)	Fermi level (eV)
CNT(10,0)				−4.55
CNT−H_2O	−0.023		0.002	
CNT−Cl	−0.57	2.114	0.22	−5.13
CNT−Cl−H_2O	−0.67	2.305	0.34	−5.43
CNT−Cl−$2H_2O$	−0.87	2.727	0.44	−5.73

associated with the water molecules. More charges are localized in the Cl atom surrounded by water molecules, as shown in Figure 4d. Note that the C−Cl bond length increases as more charges are localized on the Cl atom. With increasing numbers of water molecules, the amount of charge transfer from the CNT to the Cl atom increases and the Fermi level is further downshifted (Figure 4e). The Fermi level shift with respect to the amount of charge transfer is −2.65 eV/electron, which is much larger than that (−1.98 eV/electron) in the absence of water molecules. The larger Fermi level shift is due to a water-assisted phenomenon. The enhancement of the binding energy of the water molecules and the strong dependence of the Fermi level and the charge transfer on water content may be advantageous for sensing humidity. We also calculated the effect of O_2 and N_2 on the CNT−Cl structure to test selective response from water adsorption. The change of properties of CNT−Cl structure was negligible when O_2 and N_2 were adsorbed on CNT−Cl (Supporting Information Figure S4). This explains why CNT doped by $AuCl_3$ is not sensitive with O_2 and N_2.

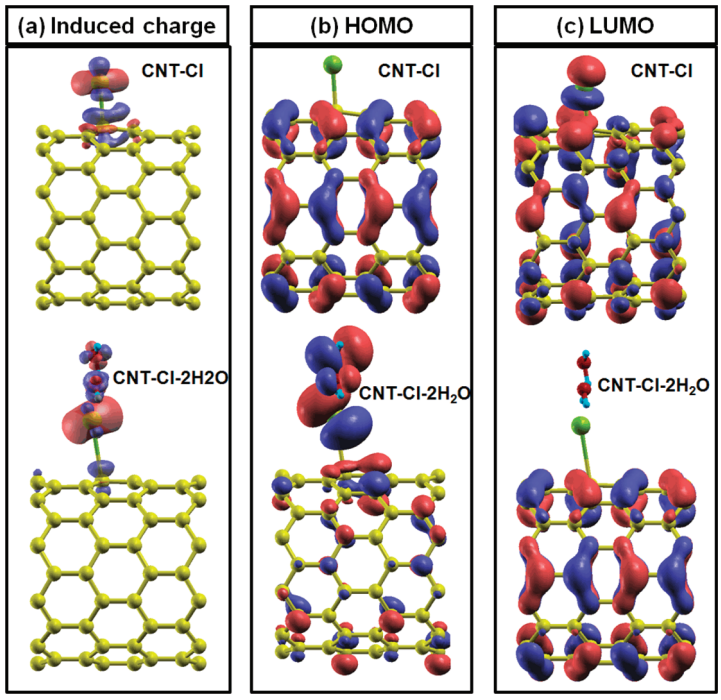

Figure 5. (a) Induced charge densities, (b) HOMO, and (c) LUMO of CNT−Cl (top) and CNT−Cl−$2H_2O$ (bottom) structure. The red (blue) in panel a indicates charge accumulation (depletion), where the values of the red and blue surfaces are ±0.003 eÅ^{-3}. (b) HOMO and (c) LUMO charge densities where the different colors indicate the wave function sign. The isovalue of HOMO and LUMO is 0.02.

To understand the nature of the bonding between carbon and chlorine atoms, we calculated the induced charge density, as shown in Figure 5a. The induced charge was defined as $\rho_{induced} = \rho_{CNT-Cl} - \rho_{Cl} - \rho_{CNT}$. In the case of Cl adsorption, the accumulated charge density (red) is strongly localized at the chlorine atom, while the depleted charge density (blue) is between two Cl atoms and a carbon atom in the CNT. This indicates that the covalent bonding character is reduced while the ionic bonding character is increased. The lowest unoccupied molecular orbital (LUMO) is localized in the Cl atom, whereas the highest occupied molecular orbital (HOMO) is localized mostly in the CNT, as shown in the top charge density images in Figure 5b,c. This is in good agreement with the analysis shown in Figure 1. Because of the partial ionic nature of this bonding, the p-type CNT−Cl structure is very sensitive to water molecules with electric dipole moments. In the case of water molecule adsorption, more charges are localized on the Cl atom, as shown in the bottom panel in Figure 5a. The HOMO in this case is mostly located in the Cl and water molecules, whereas the LUMO is primarily in the CNT. Finally, we considered the effect of water solvent in the Cl-doped CNT structure using the conductor-like screening model (COSMO).[30,31] The C−Cl bond length increased to 3.35 Å, and the amount of charge transfer to the chlorine atom was −0.87 e, which is attributed to the increased charge screening from the dielectric solution environment. It is also interesting to see how the bond angle is distorted with Cl adsorption under moisture environment. Even though sp^3 hybridization (bond angle of carbon back-bond is 116°) was increased due to Cl adsorption, as shown in Figure 1, additional water adsorption near the Cl atom recovers the original sp^2 hybridization (bond angle of carbon back-bond is 119°). This explains why D-band in Raman spectroscopy was not developed experimentally in spite of heavy doping of $AuCl_3$.[6]

CONCLUSIONS

In summary, we determined that the Cl−CNT and Cl−Au−CNT complexes are final redox products in p-doping of CNTs with a salt solution. This is in contrast with the general belief that only Au^{3+} reduction to neutral Au^0 plays a role in CNTs' doping. The bindings of Au atoms and Au clusters were enhanced through the formation of a Cl−Au−CNT complex. Nevertheless, the electronic properties of such complexes were not very different from those of the Cl−CNT complexes. The ionic nature of the C−Cl bond showed strong hygroscopic properties

by enhancing the adsorption of water molecules. Control of the precise anion concentration on the CNT surface may be a mechanism for the design of highly accurate humidity sensors.

CALCULATION METHODS

As a model structure, a (10,0) CNT consisting of 80 carbon atoms was used as a supercell. The size of our unit cell is 30 × 30 × 8.52 Å^3. The large vacuum region in the *x* and *y* directions deters interactions with neighboring CNTs as well as molecules in a different unit cell. A double numerical plus polarization basic set was employed.[24] All calculations were performed using the Perdew−Burke−Ernzerhof generalized gradient approximation (GGA) function for exchange and correlation implemented in the Dmol3 package.[25] The Brillouin zone was sampled with a 1 × 1 × 4 irreducible Monkhorst−Pack *k*-point grid for structural relaxation and a 1 × 1 × 9 grid for the electronic density of states with 0.02 eV of Gaussian smearing value.[26] The convergence in the energy was checked with a more refined grid. An orbital cutoff of 4 Å was used for all atoms, and the convergence threshold for calculation of the self-consistent energy was 10^{-6} Ry. Our model structures were relaxed until the atomic forces on the atoms were less than than 0.05 eV/Å. Different amounts of chlorine atoms were introduced to consider the concentration effect, and H_2O molecules were introduced near the Cl atoms to determine the sensitivity of the CNT−Cl structure to humidity. The effect of cell size was also checked by doubling the cell size along the *z* direction. The binding energy of the water molecule on the CNT was changed by only 4 meV, which is a 4% difference.

Because Dmol3 has accuracy issues for the calculations of spin system, we used VASP with the plane wave basic set and OPENMX with the numerical atomic basic set packages to perform spin polarization calculations.[27] The similar parameters of convergence energy threshold and *k*-point grid were used. The projector-augmented waves (PAW) and Vanderbilt ultrasoft pseudopotentials with an energy cutoff of 500 eV and 150 Ry were used in VASP and OPENMX, respectively. No spin magnetic moments were found in the CNT−Cl structures in all codes. All of the CNT−Au−Cl complex structures were optimized by VASP code.

Acknowledgment. This work was supported by grants from MEST through the STAR faculty project, the WCU program through KOSEF funded by MEST (R31-2008-000-10029-0), and the Industrial Technology Development Program (10031734) of the Ministry of Knowledge Economy (MKE) of Korea.

Supporting Information Available: Figures S1−S6. This material is available free of charge *via* the Internet at http://pubs.acs.org.

REFERENCES AND NOTES

1. Jorio, A.; Dresselhaus, G. In *Carbon Nanotubes, Advanced Topics in the Synthesis, Structure, Properties and Applications*; Dresselhaus, M. S., Ed.; Springer: Berlin, 2008.
2. Zhang, T.; Mubeen, S.; Myung, N. V.; Deshusses, M. Recent Progress in Carbon Nanotube-Based Gas Sensors. *Nanotechnology* **2008**, *19*, 332001–332015.
3. Duclaux, L. Review of the Doping of Carbon Nanotubes (Multiwalled and Single-Walled). *Carbon* **2002**, *40*, 1751–1764.
4. Snow, E. S.; Perkins, F. K.; Robinson, J. A. Chemical Vapor Detection Using Single-Walled Carbon Nanotubes. *Chem. Soc. Rev.* **2006**, *35*, 790–798.
5. Geng, H. Z.; Kim, K. K.; So, K. P.; Lee, Y. S.; Chang, Y.; Lee, Y. H. Effect of Acid Treatment on Carbon Nanotube-Based Flexible Transparent Conducting Films. *J. Am. Chem. Soc.* **2007**, *129*, 7758–7759.
6. Kim, K. K.; Bae, J. J.; Park, H. K.; Kim, S. M.; Geng, H. Z.; Park, K. A.; Shin, H. J.; Yoon, S. M.; Benayad, A.; Choi, J. Y.; *et al.* Fermi Level Engineering of Single-Walled Carbon Nanotubes by $AuCl_3$ Doping. *J. Am. Chem. Soc.* **2008**, *130*, 12757–12761.
7. Tasis, D.; Tagmatarchis, N.; Bianco, A.; Prato, M. Chemistry of Carbon Nanotubes. *Chem. Rev.* **2006**, *106*, 1105–1136.
8. Belz, T.; Baue, A.; Find, J.; Gunter, M.; Herein, D.; Mockel, H.; Pfander, N.; Sauer, H.; Schulz, G.; Schutze, J.; *et al.* Structural and Chemical Characterization of N-Doped Nanocarbons. *Carbon* **1998**, *36*, 731–741.
9. Shin, H. J.; Kim, S. M.; Yoon, S. M.; Benayad, A.; Kim, K. K.; Kim, S. J.; Park, H. K.; Choi, J. Y.; Lee, Y. H. Tailoring Electronic Structures of Carbon Nanotubes by Solvent with Electron-Donating and -Withdrawing Groups. *J. Am. Chem. Soc.* **2008**, *130*, 2062–2066.
10. Kang, B. R.; Yu, W. J.; Kim, K. K.; Park, H. K.; Kim, S. M.; Park, J.; Kim, G.; Shin, H. J.; Kim, U. J.; Lee, E. H.; *et al.* Restorable Type Conversion of Carbon Nanotube Transistor Using Pyrolytically Controlled Antioxidizing Photosynthesis Coenzyme. *Adv. Funct. Mater.* **2009**, *19*, 2553–2559.
11. Kim, S. M.; Jang, J. H.; Kim, K. K.; Park, H. K.; Bae, J. J.; Yu, W. Y.; Lee, I. H.; Kim, G.; Duong, D. L.; Kim, U. J.; *et al.* Reduction-Controlled Viologen in Bisolvent as an Environmentally Stable n-Type Dopant for Carbon Nanotubes. *J. Am. Chem. Soc.* **2009**, *131*, 327–332.
12. Kim, K. K.; Yoon, S. M.; Park, H. K.; Shin, H. J.; Kim, S. M.; Bae, J. J.; Cui, Y.; Kim, J. M.; Choi, J. Y.; Lee, Y. H. Doping Strategy of Carbon Nanotubes with Redox Chemistry. *New J. Chem.* **2010**, DOI: 10.1039/c0nj00138d.
13. Zhao, J.; Lu, J. P.; Han, J.; Yang, C. K. Noncovalent Functionalization of Carbon Nanotubes by Aromatic Organic Molecules. *Appl. Phys. Lett.* **2003**, *82*, 3746–3748.
14. Giannozzi, P. Comment on "Noncovalent Functionalization of Carbon Nanotubes by Aromatic Organic Molecules". *Appl. Phys. Lett.* **2004**, *84*, 3936–3937.
15. Choi, H. C.; Shim, M.; Bangsaruntip, S.; Dai, H. Spontaneous Reduction of Metal Ions on the Sidewalls of Carbon Nanotubes. *J. Am. Chem. Soc.* **2002**, *124*, 9058–9059.
16. Goldoni, A.; Larciprete, R.; Petaccia, L.; Lizzit, S. Single-Wall Carbon Nanotube Interaction with Gases: Sample Contaminants and Environmental Monitoring. *J. Am. Chem. Soc.* **2003**, *125*, 11329–11333.
17. Kim, W.; Javey, A.; Vermesh, O.; Wang, Q.; Li, J.; Dai, H. Hysteresis Caused by Water Molecules in Carbon Nanotube Field-Effect Transistors. *Nano Lett.* **2003**, *3*, 193–198.
18. Na, P. S.; Kim, H.; So, H. M.; Kong, K. J.; Chang, H.; Ryu., B. H.; Choi, Y.; Lee, J.; Kim, B. K.; Kim, J. J.; *et al.* Investigation of the Humidity Effect on the Electrical Properties of Single-Walled Carbon Nanotube Transistors. *Appl. Phys. Lett.* **2005**, *87*, 093101–093103.
19. Zahab, A.; Spina, L.; Poncharal, P. Water-Vapor Effect on the Electrical Conductivity of a Single-Walled Carbon Nanotube Mat. *Phys. Rev. B* **2000**, *62*, 10000–10003.
20. Pati, R.; Zhang, Y.; Nayak, S. K. Effect of H_2O Adsorption on Electron Transport in a Carbon Nanotube. *Appl. Phys. Lett.* **2002**, *81*, 2638–2640.
21. Tang, D.; Ci, L.; Zhou, W.; Xie, S. Effect of H_2O Adsorption on the Electrical Transport Properties of Double-Walled Carbon Nanotubes. *Carbon* **2006**, *44*, 2155–2159.
22. Peng, S.; Cho, K. Chemical Control of Nanotube Electronics. *Nanotechnology* **2000**, *11*, 57–60.
23. Sung, D.; Hong, S.; Kim, Y. H.; Park, N.; Kim, S.; Maeng, S. L.; Kim, K. C. *Ab Initio* Study of the Effect of Water Adsorption on the Carbon Nanotube Field-Effect Transistor. *Appl. Phys. Lett.* **2006**, *89*, 243110–243112.
24. Delley, B. An All-Electron Numerical Method for Solving the Local Density Functional for Polyatomic Molecules. *J. Chem. Phys.* **1990**, *92*, 508–517.
25. Perdew, J. P.; Burke, K.; Ernzerhof, M. Generalized Gradient Approximation Made Simple. *Phys. Rev. Lett.* **1996**, *77*, 3865–3868.

26. Monkhorst, H.; Pack, J. D. Special Points for Brillouin-Zone Integrations. *Phys. Rev. B* **1976**, *13*, 5188–5192.
27. Available on its web page (http://www.openmx-square.org/); G. Kresse and J. Furthmüller (http://cms.mpi.univie.ac.at/vasp).
28. Pan, H.; Feng, Y. P.; Lin, J. Y. *Ab Initio* Study of F- and Cl-Functionalized Single Wall Carbon Nanotubes. *J. Phys: Condens. Matter* **2006**, *18*, 5175–5184.
29. Lee, I. H.; Kim, U. J.; Son, H. B.; Yoon, S.-M.; Yao, F.; Yu, W. J.; Duong, D. L.; Choi, J. Y.; Kim, J. M.; Lee, E. H.; *et al.* Hygroscopic Effects on $AuCl_3$-Doped Carbon Nanotubes. *J. Phys. Chem. C* **2010**, *114*, 11618–11622.
30. Klamt, A.; Schüürmann, G. COSMO: A New Approach to Dielectric Screening in Solvents with Explicit Expressions for the Screening Energy and Its Gradient. *J. Chem. Soc., Perkin Trans. 2* **1993**, 799–805.
31. Delley, B. The Conductor-like Screening Model for Polymers and Surfaces. *Mol. Simul.* **2006**, *32*, 117–123.
32. Atkins, P.; Jones, L. *Chemical Principles-The Quest for Insight*, 4th ed.; W.H. Freeman and Company, New York, 2007.
33. Bendiab, N.; Almairac, R.; Rols, S.; Aznar, R.; Sauvajol, J. L.; Mirebeau, I. Single-Walled Carbon Nanotube Growth from a Cap Fragment on an Iron Nanoparticle: Density-Functional Tight-Binding Molecular Dynamics Simulations. *Phys. Rev. B* **2004**, *69*, 195415–195421.
34. Park, N.; Sung, D.; Hong, S.; Kang, D.; Park, W. Metallization of the Semiconducting Carbon Nanotube by Encapsulated Bromine Molecules. *Physica E* **2005**, *29*, 693–697.
35. Choi, W. I.; Ihm, J.; Kim, G. Modification of the Electronic Structure in a Carbon Nanotube with the Charge Dopant Encapsulation. *Appl. Phys. Lett.* **2008**, *92*, 193110–193112.
36. Michelson, E. T.; Huffman, C. B.; Rinzler, A. G.; Smalley, R. E.; Hauge, R. H.; Margrave, J. L. Fluorination of Single-Wall Carbon Nanotubes. *Chem. Phys. Lett.* **1998**, *296*, 188–194.
37. Touhara, H.; Okino, F. Property Control of Carbon Materials by Fluorination. *Carbon* **2000**, *38*, 241–267.